BIOCHEMISTRY
including biophysical chemistry & molecular biology

Rapid Report

pubs.acs.org/biochemistry

Difference in Fibril Core Stability between Two Tau Four-Repeat Domain Proteins: A Hydrogen−Deuterium Exchange Coupled to Mass Spectrometry Study

Gayathri Ramachandran[†] and Jayant B. Udgaonkar*

National Centre for Biological Sciences, Tata Institute of Fundamental Research, Bangalore 560 065, India

Supporting Information

ABSTRACT: One of the signatures of Alzheimer's disease and tauopathies is fibrillization of the microtubule-associated protein tau. The purpose of this study was to compare the high-resolution structure of fibrils formed by two different tau four-repeat domain constructs, tau4RD and tauK18, using hydrogen−deuterium exchange coupled to mass spectrometry as a tool. While the two fibrils are found to be constructed on similar structural principles, the tauK18 fibril has a slightly more stable core. This difference in fibril core stability appears to be reflective of the mechanistic differences in the aggregation pathways of the two proteins.

The aggregation of the microtubule-associated protein tau into amyloid fibrils is associated with both Alzheimer's disease and the neurodegenerative tauopathies. The protein tau has at the C-terminus three or four repeats (3R or 4R, respectively) that constitute the core of the microtubule-binding domain. Mechanistic and structural studies that seek to understand the fibrillization process *in vitro* in the hope that this knowledge will aid drug discovery use either the full-length tau isoforms, composed of both N- and C-terminal domains, or truncated tau 3R or 4R domain constructs to study the aggregation process.[1] The basic mechanism of tau aggregation in the presence of inducers has been described by several studies as ligand-induced nucleation-dependent polymerization (NDP).[2,3] Several high-resolution structural studies have also determined that of the four repeat sequences, the core of tau fibrils is built by the second and third repeats (R2 and R3, respectively)[4,5] (Figure S1 of the Supporting Information). Previous work from our laboratory examined the aggregation mechanism of two different tau 4R domain constructs, tau4RD and tauK18, in the presence of the ligand/inducer heparin.[6,7] Tau4RD has 14 additional residues at the C-terminus compared to tauK18 (Figure S1 of the Supporting Information). While the basic aggregation mechanism of both constructs could be described as ligand-induced NDP, there were important differences in terms of the nature of parallel pathways that were also available for aggregation. For tau4RD aggregation, the parallel pathway is unproductive for fibril formation but leads instead to the formation of protofibrils and nonfibrillar aggregates,[6] while for tauK18 aggregation, the parallel pathway is productive and allowed by fibril fragmentation on the main pathway for fibril growth.[7] The final mature fibrils formed by both constructs are predominantly thin fibrils,[6,7] with a few thick fibrils similar to the paired helical filaments, seen prominently in the case of tau4RD.[6,8] The final structures of the fibrils formed by the two constructs also cannot be distinguished by Fourier transform infrared spectroscopy.[6,7] In this context, the primary purpose of this study was to determine if the mechanistic differences in tau 4R domain aggregation would manifest themselves in differences in the high-resolution structures of the fibrils as measured using hydrogen−deuterium exchange coupled to mass spectrometry (HDX−MS).

Tau4RD and tauK18 were expressed and purified as described previously.[6,7] Fibrillization reactions for the mapping of the fibril core by HDX−MS were set up at a protein concentration of 100 μM. Aggregation conditions for both constructs were identical: 25 mM Tris buffer (pH 7), 50 mM NaCl, 2 mM dithiothreitol, and 37.5 μM inducer heparin. Deuterium labeling was conducted for 15 min at 37 °C in 25 mM Tris buffer (pD 7) and 50 mM NaCl, made in D_2O. Labeled fibril samples were disaggregated and quenched using 2 M guanidine hydrochloride (GdnHCl) and 100 mM glycine buffer (pH 2.5) and desalted using ice-cold water (pH 2.5); the samples were then injected into the HDX module of the Synapt G2 HD mass spectrometer (Waters). Fibril cores were mapped with the aid of peptide maps that were generated by pepsin digestion. Monomeric samples of both tau4RD and tauK18 were processed like the fibril samples to control for back and forward exchange during HDX−MS. This allowed for the determination of the extent of deuterium incorporation for each of the peptides (see the Supporting Information for details).

Peptide maps were generated for both tau four-repeat domain constructs by controlled proteolysis using pepsin at low pH. The peptides used in this study are shown in Figure S1 of the Supporting Information. For tau4RD, the map consists of 17 overlapping peptides that cover ∼95% of the protein sequence, while for tauK18, it consists of 16 overlapping peptides that cover ∼97% of the protein sequence. The peptides generated for both constructs are the same, except at the C-terminus where the presence of 14 additional residues in tau4RD compared to tauK18 results in two different peptides (Figure S1 of the Supporting Information). More importantly, the level of coverage obtained was sufficient to map the core of the two fibrils (see below).

Received: October 23, 2013
Revised: November 18, 2013
Published: November 20, 2013

   dx.doi.org/10.1021/bi4014352 | *Biochemistry* 2013, 52, 8787−8789

Figure 1 shows mass spectra of four select peptide fragments that are representative of the four repeat regions of tau, obtained

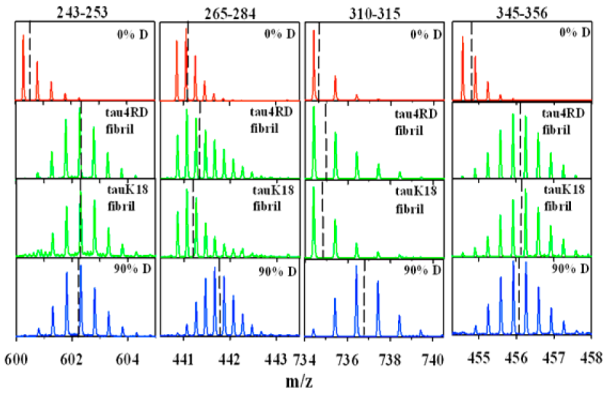

Figure 1. Mass spectra of selected peptides that span the four repeat sequences of tau obtained following HDX from tau4RD and tauK18 fibrils for 15 min. The mass spectra of the appropriate controls, namely, protonated (0% D) and deuterated (90% D) peptides derived from tau4RD, are also shown (the data for 0 and 90% D peptides are not significantly different for tau4RD and tauK18). The dashed lines represent the centroid average m/z for a particular peptide.

following deuterium labeling of both tau4RD and tauK18 fibrils for 15 min. As one may see, the mass spectra show unimodal isotopic m/z envelopes consistent with each peptide fragment existing in one predominant conformation. Further, different peptide fragments exhibit different extents of deuterium incorporation as measured by the position of the centroid average m/z of the fibrils relative to that of the protonated (0% D) and fully deuterated (90% D) controls (see the dashed lines in Figure 1). These differences arise from the differences in the structural content of the sequence segments that correspond to the peptide fragments: segments that are in structured β-sheets will show little deuterium incorporation upon HDX, while those that are found in disordered turns or loops will easily exchange their amide hydrogen for deuterium and will hence exhibit substantial deuterium incorporation.[9] For tau4RD and tauK18 fibrils, the sequence segment 265−284 that largely corresponds to repeat R2 and the sequence segment 310−315 that corresponds to repeat R3 are protected from HDX, indicative of their participation in the fibril core (Figure 1). In contrast, sequence segments 243−253 and 345−356, corresponding to repeats R1 and R4, respectively, are accessible to HDX, indicative of the solvent exposure of these fibrillar regions (Figure 1).

This pattern of protection against HDX for the whole of tau4RD and tauK18 fibrils is shown in Figure 2. At first glance, the core regions of the two fibrils appear to be largely similar. The region that shows the strongest protection (<25% D incorporation) is found in repeat R3, while a separate region of moderate protection (25−75% D incorporation) is found in repeat R2 (Figure 2 and Figure S2 of the Supporting Information). This view of the fibril core formed by the tau four-repeat domain is consistent with results obtained from electron paramagnetic resonance (EPR) studies of the full-length 2N4R (two inserts at the N-terminus and 4R at the C-terminus) tau isoform[5,10] and a HDX−nuclear magnetic resonance (NMR) study of tauK18 fibrils.[4] The HDX-protected core region of repeat R3 appears to be composed of two segments: a strongly protected core that extends over residues V306−L315 and a moderately protected core region that extends over residues

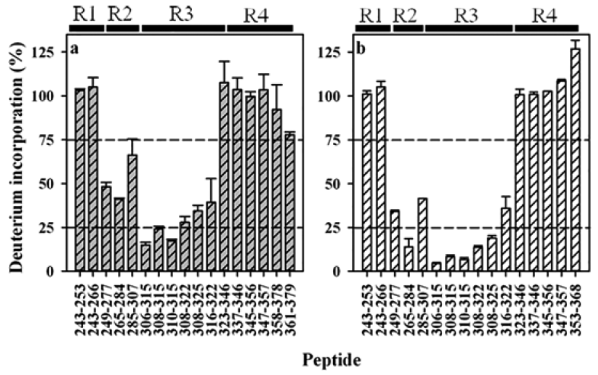

Figure 2. Extent of incorporation of deuterium into different sequence segments of (a) tau4RD fibrils and (b) tauK18 fibrils following HDX for 15 min. The percent deuterium incorporation for each peptide fragment was calculated as described above. The error bars represent the standard deviations calculated from two independent experiments. The dashed lines are used to define protection thresholds: strongly protected (<25% D), moderately protected (25−75% D), and weakly protected (>75% D).

S316−C322 (Figure 2 and Figure S2 of the Supporting Information). This structure is very similar to the structure proposed for one of two populations of coexisting tauK19 (3R domain construct) fibrils from a recent solid-state NMR study, in which the secondary chemical shift data indicated the presence of two β-strands that extended over V306−L315 (with a kink at P312) and a third β-strand that extended over K317−C322 (with kinks at S316 and G323).[4] Indeed, an EPR study of 2N4R tau fibrils also identified L315 as the site of a possible turn conformation.[5] Additionally, the HDX−NMR data for tauK18 and tauK19 fibrils also concur with respect to the remarkable similarity in the organization of repeat R3 in the two different fibrils.[4] The protection against HDX for repeat R2 (unique to the four-repeat constructs) in the tau4RD and tauK18 fibrils examined in this study indicates the existence of a distinct region of moderate protection (Figure 2 and Figure S2 of the Supporting Information). In contrast, repeats R1 and R4 are completely solvent-exposed except for a short stretch in repeat R1 (K267−K274) that is possibly structured (Figure 2 and Figure S2 of the Supporting Information).

A careful examination of the strongly protected core (V306−L315) in repeat R3 of both tau4RD and tauK18 fibrils reveals an interesting detail (Figure 2). Both tau4RD and tauK18 fibrils display a gradation in the protection pattern of the ^{306}VQIVYK^{311} hexapeptide motif. The HDX−MS data of peptides that correspond to sequence segments 306−315, 308−315, and 310−315 indicate that residues I308 and V309 are less protected than the two flanking residues on either side, in both tau4RD and tauK18 fibrils (Figure 2). Quite surprisingly, an opposite graded pattern of protection can be seen in the HDX−NMR data of tauK18 fibrils, though this pattern is not mentioned in that study; in that data set, residues I308 and V309 are more protected than the two flanking residues on either side.[4]

More crucially perhaps for the purpose of this study, there appears to be a subtle difference in the stabilities of the fibril cores of tau4RD and tauK18, as measured by a difference in the magnitude of deuterium incorporation (Figure 2). The sequence segment 310−315 belonging to repeat R3, for example, shows 17% D incorporation (Figure 2a) in tau4RD fibrils versus 7% D in tauK18 fibrils (Figure 2b). This difference in stability exists in repeat R2, as well: the sequence segment 285−307 shows 66% D

dx.doi.org/10.1021/bi4014352 | Biochemistry 2013, 52, 8787−8789

incorporation in tau4RD fibrils (Figure 2a) as opposed to 42% D incorporation in tauK18 fibrils (Figure 2b), while the sequence segment 265−284 shows 40% D incorporation in tau4RD fibrils (Figure 2a) as opposed to 14% D incorporation in tauK18 fibrils (Figure 2b). This subtle difference in stability is recapitulated by a different measure of structural integrity, namely, the kinetics of fibrillar disaggregation (Figure S3a of the Supporting Information). When tau4RD and tauK18 fibrils were diluted identically into 2 M GdnHCl, Tris buffer (pH 7), 98 and 70% of tau4RD and tauK18 fibrils, respectively, disaggregated within the mixing dead time (Figure S3a of the Supporting Information). While the rapid disaggregation kinetics does not allow for a robust quantitation of the disaggregation rate, because only a small fraction of the process can be measured, the slower disaggregation of tauK18 fibrils (Figure S3a of the Supporting Information) corroborates effectively the observation from HDX−MS measurements that the stability of tauK18 fibrils is slightly greater than that of tau4RD.

This is the first study to have used HDX−MS to map the core of tau fibrils and to compare the fibril cores of two tau 4R domain constructs that form fibrils by slightly different mechanisms. Although the aggregation mechanisms of both constructs satisfy the basic tenets of ligand-induced NDP, mechanistic differences exist at the level of the operation of additional pathways for fibrillization (see above). The main result of this study is the observation that although the sequence segments that participate in the construction of the fibril core are the same for both constructs, the stability of the tauK18 fibril formed by means of both a primary and a secondary pathway for fibril growth is greater than that of the tau4RD fibril (Figure 2). It is also tempting to speculate that the presence of 14 additional residues in tau4RD that are predominantly positively charged (Figure S1 of the Supporting Information) weakens the tau4RD fibril core, potentially by interfering with electrostatic interactions in the core. Proof of this hypothesis would require, however, higher-resolution data about the three-dimensional structure of the fibril cores; hence, this remains an interesting future avenue of research.

A final interesting correlation is worthy of note. The amplitude of ThT fluorescence for the same molar concentration of fibrils is ∼2-fold greater for tauK18 than for tau4RD.[6,7] Another characteristic of amyloid fibrils that was discovered recently is a diagnostic intrinsic fluorescence that fibrils are found to emit,[11] purported to arise from the extensive hydrogen bonding network that holds together the β-strands of amyloid fibrils.[12] Indeed, the intrinsic fluorescence spectra of both tau4RD and tauK18 amyloid fibrils acquired with fluorescence excitation at 405 nm show an emission peak at 450 nm (Figure S3b of the Supporting Information), similar to that seen in previous studies.[13] It appears possible that the intensity of the intrinsic fluorescence emission, in addition to the position of the emission peak, will be a feature that will distinguish different fibrils and be indicative of differences in hydrogen bonding.[13] Indeed, it is seen that the intensity of the intrinsic fluorescence emission at 450 nm is ∼2-fold greater for tau4RD than for tauK18 fibrils (Figure S3b of the Supporting Information), although both fibrils show an increase in intrinsic fluorescence intensity compared to that of the monomer. A comparison of these values in light of the results of the HDX−MS study leads us to postulate that an inverse correlation of ThT fluorescence intensity with the intrinsic fluorescence intensity is potentially reflective of an underlying difference in fibril core stability.

■ ASSOCIATED CONTENT

Supporting Information

Detailed experimental procedures and Figures S1−S3. This material is available free of charge via the Internet at http://pubs.acs.org.

■ AUTHOR INFORMATION

Corresponding Author

*E-mail: jayant@ncbs.res.in. Telephone: 91-80-23666150. Fax: 91-80-23636662.

Present Address

†G.R.: Department of Molecular Biosciences, Northwestern University, Evanston, IL 60208.

Funding

This work was funded by the Tata Institute of Fundamental Research and the Department of Biotechnology, Government of India. G.R. was a recipient of the S. P. Mukherjee fellowship from the Council of Scientific and Industrial Research, Government of India, at the beginning of this work. J.B.U. is a recipient of the J. C. Bose National fellowship from the Government of India.

Notes

The authors declare no competing financial interests.

■ ACKNOWLEDGMENTS

We thank John Engen for e-mail advice on dealing with carryover on the immobilized pepsin column and Jogender Singh for assistance with figures.

■ REFERENCES

(1) Ramachandran, G., and Udgaonkar, J. B. (2013) *Biochemistry 52*, 4107−4126.

(2) Friedhoff, P., von Bergen, M., Mandelkow, E. M., Davies, P., and Mandelkow, E. (1998) *Proc. Natl. Acad. Sci. U.S.A. 95*, 15712−15717.

(3) King, M. E., Ahuja, V., Binder, L. I., and Kuret, J. (1999) *Biochemistry 38*, 14851−14859.

(4) Daebel, V., Chinnathambi, S., Biernat, J., Schwalbe, M., Habenstein, B., Loquet, A., Akoury, E., Tepper, K., Muller, H., Baldus, M., Griesinger, C., Zweckstetter, M., Mandelkow, E., Vijayan, V., and Lange, A. (2012) *J. Am. Chem. Soc. 134*, 13982−13989.

(5) Margittai, M., and Langen, R. (2004) *Proc. Natl. Acad. Sci. U.S.A. 101*, 10278−10283.

(6) Ramachandran, G., and Udgaonkar, J. B. (2011) *J. Biol. Chem. 286*, 38948−38959.

(7) Ramachandran, G., and Udgaonkar, J. B. (2012) *J. Mol. Biol. 421*, 296−314.

(8) Wegmann, S., Jung, Y. J., Chinnathambi, S., Mandelkow, E. M., Mandelkow, E., and Muller, D. J. (2010) *J. Biol. Chem. 285*, 27302−27313.

(9) Englander, S. W., Sosnick, T. R., Englander, J. J., and Mayne, L. (1996) *Curr. Opin. Struct. Biol. 6*, 18−23.

(10) Margittai, M., and Langen, R. (2006) *J. Biol. Chem. 281*, 37820−37827.

(11) Chan, F. T., Kaminski Schierle, G. S., Kumita, J. R., Bertoncini, C. W., Dobson, C. M., and Kaminski, C. F. (2013) *Analyst 138*, 2156−2162.

(12) Shukla, A., Mukherjee, S., Sharma, S., Agrawal, V., Radha Kishan, K. V., and Guptasarma, P. (2004) *Arch. Biochem. Biophys. 428*, 144−153.

(13) Pinotsi, D., Buell, A. K., Dobson, C. M., Kaminski Schierle, G. S., and Kaminski, C. F. (2013) *ChemBioChem 14*, 846−850.